Bone Marrow-Derived Mesenchymal Stem Cells-Derived Exosomes Promote Survival of Retinal Ganglion Cells Through miRNA-Dependent Mechanisms

Ben Mead, Stanislav Tomarev

Key Words. Mesenchymal stem cells • Retinal ganglion cells • Exosomes • Optic nerve crush • Neuroprotection

Section of Retinal Ganglion Cell Biology, Laboratory of Retinal Cell and Molecular Biology, National Eye Institute, National Institutes of Health, Bethesda, Maryland, USA

Correspondence: Ben Mead, BSc, MRes, PhD, Section of Retinal Ganglion Cell Biology, Laboratory of Retinal Cell and Molecular Biology, National Eye Institute, National Institutes of Health, Bethesda, Maryland 20892, USA. Telephone: 301-402-4506; Fax: 301-480-2610; e-mail: ben.mead@nih.gov or Stanislav Tomarev, Section of Retinal Ganglion Cell Biology, Laboratory of Retinal Cell and Molecular Biology, National Eye Institute, National Institutes of Health, Bethesda, Maryland 20892, USA. Telephone: 301-496-8524; Fax: 301-480-2610; e-mail:tomarevs@nei.nih.gov

Abstract

The loss of retinal ganglion cells (RGC) and their axons is one of the leading causes of blindness and includes traumatic (optic neuropathy) and degenerative (glaucoma) eye diseases. Although no clinical therapies are in use, mesenchymal stem cells (MSC) have demonstrated significant neuroprotective and axogenic effects on RGC in both of the aforementioned models. Recent evidence has shown that MSC secrete exosomes, membrane enclosed vesicles (30–100 nm) containing proteins, mRNA and miRNA which can be delivered to nearby cells. The present study aimed to isolate exosomes from bone marrow-derived MSC (BMSC) and test them in a rat optic nerve crush (ONC) model. Treatment of primary retinal cultures with BMSC-exosomes demonstrated significant neuroprotective and neuritogenic effects. Twenty-one days after ONC and weekly intravitreal exosome injections; optical coherence tomography, electroretinography, and immunohistochemistry was performed. BMSC-derived exosomes promoted statistically significant survival of RGC and regeneration of their axons while partially preventing RGC axonal loss and RGC dysfunction. Exosomes successfully delivered their cargo into inner retinal layers and the effects were reliant on miRNA, demonstrated by the diminished therapeutic effects of exosomes derived from BMSC after knockdown of Argonaute-2, a key miRNA effector molecule. This study supports the use of BMSC-derived exosomes as a cell-free therapy for traumatic and degenerative ocular disease. Stem Cells Translational Medicine 2017;6:1273–1285

Significance Statement

The dysfunction and loss of retinal ganglion cells (RGC), such as seen with glaucoma and traumatic optic neuropathy is a major cause of blindness. While mesenchymal stem cells (MSC) have a demonstrable neuroprotective effect at protecting RGC, ideally the active components would be purified and delivered in a cell-free manner. Here we show that exosomes, small extracellular vesicles secreted from MSC can be easily purified from MSC and, when delivered into a rodent model of optic nerve crush, protect RGC from death and preserve function.

Introduction

Mesenchymal stem cells (MSC) are a self-replicating multipotent stromal cell isolated from mesenchymal tissues such as bone marrow (BMSC) [1], adipose [2], dental pulp [3] and umbilical cord blood [4] as well as other tissues. MSC have demonstrated therapeutic efficacy at promoting the protection and regeneration of central nervous system (CNS) neurons, which lack the capacity to regenerate, or be replaced following loss. The retina is an outgrowth of the brain and is thus part of the CNS and subject to the same regenerative limitations [5]. Retinal ganglion cells (RGC) are the sole projection neurons and their axons make up the optic nerve, making them susceptible to traumatic (optic nerve crush; ONC) and degenerative (glaucoma) diseases. Loss or dysfunction of RGC is a leading cause of irreversible blindness and the development of neuroprotective and axogenic therapies is a focus of research. We and others have demonstrated the therapeutic efficacy of MSC in models of ONC and glaucoma, in vitro and in vivo [Reviewed in [6]]. In retinal cultures, MSC proved neuroprotective and neuritogenic for injured RGC [7, 8]. After ONC, MSC transplanted into the vitreous are able to promote significant neuroprotection of RGC and moderate regeneration of their axons [9–12]. In animal models of glaucoma, MSC promote the survival of RGC and their axons and preserve their function [13–16].

Although the efficacy of MSC is well established, the mechanism by which these cells protect RGC and promote regeneration of their axons is poorly understood. Evidence strongly suggests a paracrine-mediated effect with secreted factors being necessary. In culture, MSC are efficacious when cocultured (yet physically separated) from the injured retinal cells [7]. The assumption that neurotrophic growth factors (NTF) are important is corroborated both by the expansive NTF rich secretome of MSC and by the attenuated neuroprotective and neuritogenic effects when particular NTF receptors are inhibited [7, 10]. Secreted NTF such as platelet-derived growth factor and brain-derived neurotrophic factor have been shown to be important to the neuroprotection of RGC [7, 17] whereas MSC mediated-neuritogenesis depended more on nerve growth factor [7]. Other secreted factors, such as Wnt3a have been implicated in the neuroprotective effect of MSC on CNS neurons [18]. Transplantation into the vitreous of healthy and diseased eyes yields no evidence of differentiation or migration/integration into retinal tissue [9, 10, 13, 15, 19], strongly implicating paracrine over cell replacement as the dominant mechanism.

Following on from this established paracrine-mediated mechanism, mounting evidence exists for the potential of MSC to benefit nearby injured tissues through the secretion of exosomes. Exosomes, described over 30 years ago [20], are endocytic-derived structures composed of proteins, lipids, and mRNA surrounded by a phospholipid bi-layer that are secreted into the extracellular space. Their size ranges from 30 to 100 nm although typically in the literature they are grouped with another class of extracellular vesicle (EV) known as microvesicles which range from 100 to 1,000 nm [21]. Proteomic analysis of BMSC-derived exosome contents shows that many of the factors are also found within BMSC conditioned medium [22]. Exosomes contain (along with proteins) mRNA and miRNA, which are both functional and, when delivered to another cell via fusion with the cell membrane, lead to the translation of new proteins [23]. Intercellular delivery of exosomes has now been demonstrated for a number of different cell types, all showing capacity to make functional use of the delivered miRNA [24]. Characterization of exosome uptake shows that upon delivery to donor cells, exosomes are shuttled inside endocytic vesicles and delivered to endoplasmic reticulum and lysosomes [25].

BMSC are known to secrete exosomes [26] which contain over 150 different miRNA molecules [27] that can be delivered to target cells. Various studies have shown that exosomes play a major role in the therapeutic effect BMSC provide. In the heart, BMSC conditioned medium improves cardiac function yet the active component is derived from the fraction >1,000 kda, ruling out most candidate secreted growth factors [28]. Further studies demonstrated that the treatment of mice with BMSC-derived purified exosomes is able to reduce cardiac infarct size ex vivo and in vivo [26, 29, 30]. BMSC exosomes from human, rat, and mouse have demonstrated therapeutic efficacy in a variety of other injury models, mediated through both their protein and RNA cargo [31].

Treatment of primary adult rat cortical neurons with BMSC-derived exosomes promoted neurite outgrowth, an effect that was dependent on miRNA encapsulated in exosomes [32]. Inhibition of Argonaut-2 (Ago2), a protein important in enacting the RNA interference function of miRNA attenuates the neuritogenic properties of exosomes. Intravenous administration of BMSC-derived exosomes promotes functional recovery in animals through proangiogenic and proneurogenic effects at the injury site following stroke [33] and traumatic brain injury [34]. In a mouse model of diabetes-induced cognitive impairment, BMSC-derived exosomes delivered into the cerebral ventricles promoted functional recovery [35]. Of note, exosomes actively integrated into both neurons and astrocytes.

In the present rodent study, we aimed to test the neuroprotective and axogenic potential of BMSC-derived exosomes on injured RGC in vitro and in vivo and to determine if the effect is protein or miRNA mediated.

MATERIALS AND METHODS

All reagents were purchased from Sigma (Allentown, PA, https://www.sigmaaldrich.com) unless otherwise specified.

BMSC Cultures

Human BMSC were purchased from Lonza (Walkersville, MD, http://www.lonza.com/) and represented pooled samples from three donors. The CD29$^+$/CD44$^+$/CD73$^+$/CD90$^+$/CD45$^-$ (confirmed by supplier) BMSC were seeded into T25/T75 flasks (Corning, Acton, MA, https://www.corning.com) in a total volume of 5 ml/15 ml DMEM containing 1% penicillin/streptomycin and 10% exosome-depleted foetal bovine serum (Thermo Fisher Scientific, Cincinnati, OH, https://www.thermofisher.com) and at a density of 1×10^6 cells/2×10^6 cells, respectively. Cultures were maintained at 37°C in 5% CO_2, the supplemented medium was changed every 3 days and the cells were passaged when 80% confluent using 0.05% trypsin/ EDTA to lift them from their surface attachment. For control cells, human fibroblasts were purchased from Lonza and cultured in the exact same conditions. For all experiments, BMSC and fibroblasts were used at passage 2–5.

Transfection of BMSC With siRNA

BMSC were transfected using Lipofectamine 3000 (Thermo Fisher) according to the manufacturer's protocol. Briefly, 70% confluent BMSC grown in Opti-MEM medium were incubated with Lipofectamine 3000 reagent and either siRNA against Argonaute 2 (SiAgo2) or a scrambled control siRNA (SiScr) for 48 hours.

Western Blot

Successful Ago2 knockdown was confirmed by Western blotting. Briefly, BMSC were washed in phosphate buffered saline (PBS), lysed in lysis buffer (20 mM Tris-HCl, 1 mM EDTA, 0.5 mM EGTA, 150 mM NaCl, 1% NP-40, and protease inhibitor) and sonicated before protein concentration was determined by BCA protein assay (Thermo Fisher). 20 μg total protein samples were separated on 4%–12% Bis-Tris protein gels at 150 V for 40 minutes. Proteins were transferred to polyvinylidene fluoride membranes, blocked for 30 minutes in 10% Western blocking buffer in Tris buffered saline (TBS), stained for 1 hour with primary antibody (Supporting Information Table 1) diluted in TBS, washed with TBST for 3 × 5 minutes, stained for 1 hour with secondary antibody before a final 3 × 5 minutes wash and detection with Femto ECL. Densitometry of Western blot bands was analyzed using ImageJ software (National Institutes of Health, Bethesda, MD, https://imagej.nih.gov).

Exosome Isolation

Exosomes were isolated from BMSC and fibroblasts using ultracentrifugation as previously described [21]. Briefly, BMSC/fibroblasts were cultured for 48 hours in exosome free serum and conditioned medium was collected and centrifuged at 300g for 10 minutes, 2,000g for 10 minutes and 10,000g for 30 minutes,

discarding the pellet and collecting the supernatant each time. The supernatant was spun down at 100,000g twice, each for 70 minutes, the pellet collected and resuspended in 1 ml sterile PBS (sPBS). To remove microvesicles, EV were filtered through a 0.22 μm filter to obtain exosomes. The supernatant was used as a negative control in the following step to confirm absence of exosomes. Exosomes were isolated from BMSC/fibroblasts at passage 2, up to passage 5.

Electron Microscopy

Exosomes were doubly-fixed in a PBS-buffered glutaraldehyde (2.5% at pH 7.4) and osmium tetroxide (0.5%), and embedded in epoxy resin. Thin sections (90 nm) were collected on 200-mesh copper grids, air-dried, and doubly-stained with uranyl acetate and lead citrate. Sections were viewed with a JEOL JEM-1010 electron microscope, and photographed.

Exosome Quantification

Exosomes were quantified using ExoELISA against CD63 (System Biosciences, Mountain View, CA https://www.systembio.com) according to the manufacturer's instructions. Briefly a standard curve was constructed using exosome standards and test samples of purified exosomes from BMSC and fibroblasts, run in duplicate with exosome quantity extrapolated from the standard curve.

Exosome Surface Marker Expression

The expression of surface epitopes was determined by flow cytometry using the MACSPlex Exosome Kit (human) (Cat No. 130108813 Miltenyi Biotec, Bergish Gladbach, Germany, http://www.miltenyibiotec.com) Briefly, 2×10^{10} exosomes were washed and suspended in sPBS and assayed using a MACSQuant Analyzer 10 (Miltenyi Biotec) with MACSQuantify Software Version 2.8. Assay was run in triplicate on three independent samples.

Exosome Tracking

To track exosomes in vivo, Exo-Glow (System Biosciences) was used to label purified exosomes prior to intravitreal injection, according to the manufacturer's instructions. Briefly, 3×10^8 exosomes were suspended in 500 μl of sPBS and incubated with Exo-Green labeling solution for 10 minutes at 37°C followed by 30 minutes on ice. Labeled exosomes were isolated by treatment with Exoquick-TC (System Biosciences), centrifugation for 30 minutes at 14,000g, washed three times with sPBS before being resuspended in 500 μl of sPBS and kept on ice until intravitreal injection on the same day.

Animals

Adult female Sprague-Dawley rats weighing 170–200 g (Charles River, Wilmington, MA, http://www.criver.com/) were maintained in accordance with guidelines described in the ARVO Statement for the Use of Animals in Ophthalmic and Vision Research, using protocols approved by the National Eye Institute Committee on the Use and Care of Animals.

Animals were kept at 21°C and 55% humidity under a 12 hours light and dark cycle, given food/water ad libitum and were under constant supervision from trained staff. Animals were euthanized by rising concentrations of CO_2 before extraction of retinae.

Retinal Cell Culture

Eight well chamber slides (Thermo Fisher Scientific) were pre-coated with 100 μg/ml poly-D-lysine for 60 minutes and then with 20 μg/ml laminin for 30 minutes. After culling and ocular dissection, the retinae of female Sprague-Dawley were minced in 1.25 ml of papain (20 U/ml; Worthington Biochem, Lakewood, NJ, http://www.worthington-biochem.com; as per manufacturer's instructions) containing 50 μg/ml of DNase I (62.5 μl; Worthington Biochem) and incubated for 90 minutes at 37°C. The retinal cell suspension was centrifuged at 300g for 5 minutes and the pellet resuspended in 1.575 ml of Earle's balanced salt solution (Worthington Biochem) containing 1.1 mg/ml of reconstituted albumin ovomucoid inhibitor (150 μl; Worthington Biochem) and 56 μg/ml of DNase I (75 μl). After adding to the top of 2.5 ml of albumin ovomucoid inhibitor (10 mg/ml) to form a discontinuous density gradient, the retinal cell suspension was centrifuged at 70g for 6 minutes and the cell pellet resuspended in 1 ml of supplemented Neurobasal-A (25 ml Neurobasal-A [Thermo Fisher Scientific], 1× concentration of B27 supplement [Life Technologies], 0.5 mM of L-glutamine [62.5 μl; Thermo Fisher Scientific] and 50 μg/ml of gentamycin [125 μl; Thermo Fisher Scientific]) and seeded at a density of 125,000 cells per 300 microliters per well in a 8 well chamber slide. Selected cultures were treated with BMSC/fibroblast exosomes (before and after passing through a 0.22 μm filter) or human recombinant ciliary neurotrophic factor (50 ng/ml)/ BMSC (50,000 cells) as a positive control

Cultures were incubated for 3 days at 37°C before immunocytochemical staining of RGC with βIII-tubulin. For this study, large spherical βIII-tubulin^{+} retinal cells [36], which can be identified by preferential βIII-tubulin intensity around the axonal base are referred to as RGC. Previous immunocytochemical analysis of these cultures demonstrates that 60% of these retinal cells are neurons (neurofilament[+]/βIII-tubulin[+]), of which 10% are Thy1^{+} RGC [37].

In Vivo Experimental Design

The experimental design is shown in Figure 1. Briefly, 36 adult rats were divided in the following 6 groups: Group 1, uninjured/untreated; Group 2, ONC/untreated; Group 3, ONC/BMSC-derived exosomes; Group 4, ONC/fibroblast-derived exosomes; Group 5, ONC/SiAgo2 transfected BMSC-derived exosomes; Group 6, ONC/SiScrambled transfected BMSC-derived exosomes. Only 1 eye per animal was used. ONC was performed on day 0 contemporaneously with baseline recordings of electroretinography (ERG)/optical coherence tomography (OCT). Exosome treatments were given on day 0, 7 and 14 and animals were sacrificed on day 21 following ERG/OCT measurements.

Optic Nerve Crush

Anesthesia was induced with 5% Isoflurane (Baxter Healthcare Corp, Deerfield, IL, http://www.baxter.com)/1.5 liter per minute O_2 and maintained at 3.5% throughout the procedure. Following anesthetic induction, an intraperitoneal injection of Buprenorphine (0.3 mg/kg) was administered (preoperatively) and the animal secured in a heal-holding frame. Intraorbital ONC was performed as previously described [38]. Briefly, the optic nerve was surgically exposed under the superior orbital margin and crushed using fine forceps 1 mm posterior to the lamina cribrosa, taking care to separate the dura mater and under lying retinal artery before crushing.

Intravitreal Delivery of Exosomes

Deliver of exosomes was done with a 33g Hamilton syringe (Hamilton Company, Beltsville, MD, http://www.hamiltoncompany.com/), injected into the vitreous just posterior to the limbus. A 5 μl
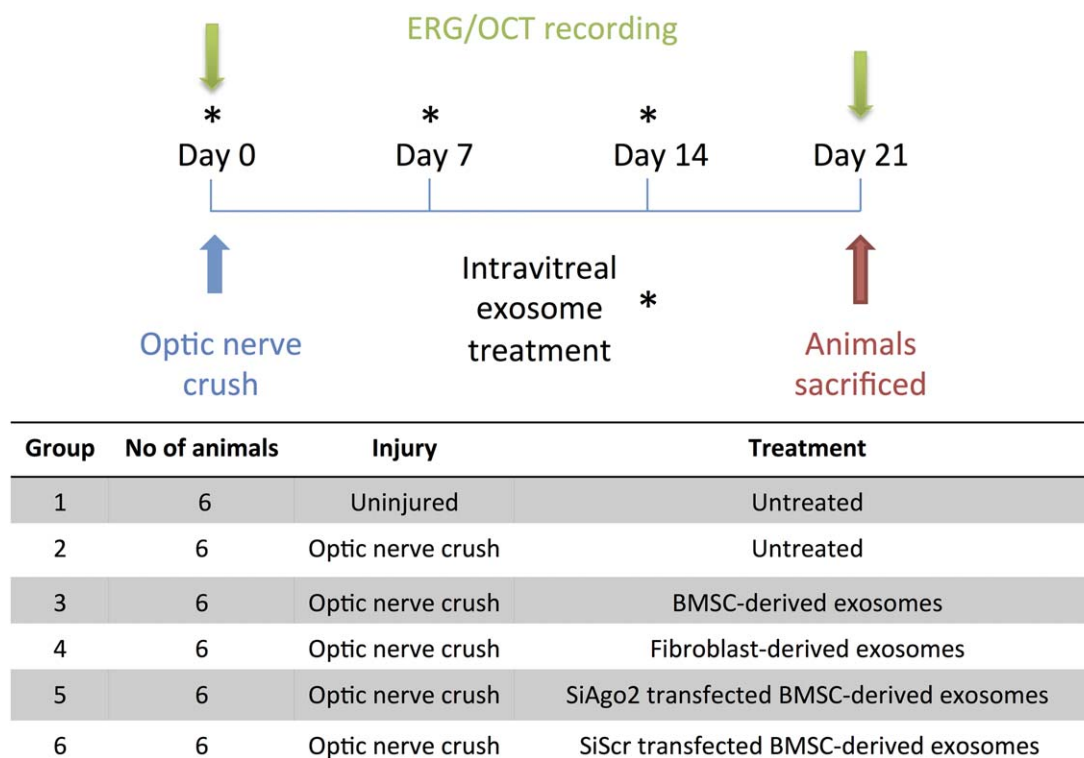
Figure 1. Experimental design of in vivo study. Timeline detailing the ERG/OCT recordings, exosome treatments and sacrifice of animals with respect to the day of the optic nerve crush surgery. The injury and treatment (*asterisks*) for each animal group is also given. Abbreviations: BMSC, bone marrow-derived mesenchymal stem cell; ERG, electroretinography; OCT, optical coherence tomography.

volume of sPBS loaded with 3×10^9 exosomes was injected slowly and the needle was retracted after 2 minutes to minimize backflow.

Electroretinography

ERG records the electrical function of retina in response to a known intensity of light, with different intensities eliciting responses in different retinal cell populations. By eliciting a RGC dependent response, visual function of the glaucomatous rats can be assessed. ERG was recorded using the Espion Ganzfeld full field system (Diagnosys LLC, Lowell, MA, http://diagnosysllc.com) before ONC (baseline) and 21 days post-ONC. Rats were dark adapted for 12 hours overnight and prepared for ERG recording under dim red light (>630 nm). Anesthesia was induced with intraperitoneal injection of Ketamine (100 mg/kg; Putney Inc, Portland, ME, http://putneyvet.com)/Xylazine (10 mg/kg; Lloyd Inc, Shenandoah, IA, http://www.lloydinc.com) and eyes dilated with tropicamide. Scotopic flash ERG were recorded from -5.5 to $+1$ log units with respect to standard flash in half log-unit steps.

ERG Analysis

ERG traces were analyzed using in built Espion software and the amplitude (with respect to baseline) was used as a measure of rat visual function. Traces at a light intensity of 1×10^{-5}mcd/s were chosen for analysis as they gave a clean, unambiguous positive scotopic threshold response (pSTR) with a mean latency of 100 ms.

OCT Measurements of the Retinal Nerve Fiber Layer

OCT was performed on rats under anesthesia (Ketamine and Xylazine, as above) pre-ONC (baseline reading) and 21 days post-ONC, before sacrifice and tissue collection. A Spectralis HRA3 confocal scanning laser ophthalmoscope (Heidelberg Engineering, Heidelberg, Germany, https://www.heidelbergengineering.com) was used to take images of the retina around the optic nerve head and in-built software segmented the retinal nerve fiber layer (RNFL) and quantified the thickness. Segmentation was manually adjusted when necessary to prevent inclusion of blood vessels that populate the RNFL.

Tissue Preparation

At 21 day post-ONC, animals were sacrificed by rising concentration of CO_2 and perfused intracardially with 4% paraformaldehyde (PFA) in PBS. Eyes and optic nerves were removed and immersion fixed in 4% PFA in PBS for 2 hours at 4°C before cryoprotection in 10, 20, and 30% sucrose solution in PBS for 24 hours with storage at 4°C. Eyes and optic nerves were then embedded using optimal cutting temperature embedding medium (VWR International Inc, Bridgeport, NJ, https://us.vwr.com) in peel-away mould containers (VWR International Inc) by rapid freezing under crushed dry ice and were stored at -80°C. After embedding, eyes and optic nerves were sectioned on a CM3050S cryostat microtome (Leica Microsystems Inc, Bannockburn, IL, http://www.leica-microsystems.com) at -22°C at a thickness of 20 µm and 14 µm, respectively, and mounted on positively charged glass slides (Superfrost Plus, Thermo Fisher Scientific). Longitudinal optic nerve and parasagittal eye sections were left to dry on slides overnight at 37°C before storage at -20°C. To ensure RGC counts were done in the same plane, eye sections were chosen with the optic nerve head visible.

Immunocytochemistry

Retinal cells were fixed in 4% PFA in PBS for 10 minutes, washed for 3×10 minutes of PBS, blocked in blocking solution (3%

bovine serum albumin (g/ml), 0.1% Triton X-100 in PBS) for 20 minutes and incubated with primary antibody (Supporting Information Table 1) diluted in antibody diluting buffer (ADB; 0.5% bovine serum albumin, 0.3% Tween 20 in PBS) for 1 hour at room temperature. Cells were then washed for 3 × 10 minutes in PBS, incubated with the secondary antibody diluted in ADB for 1 hour at room temperature, washed for 3 × 10 minutes in PBS, mounted in Vectorshield mounting medium containing DAPI (Vector Laboratories, Burlingame, CA, https://vectorlabs.com) and stored at 4°C.

Immunohistochemistry

Mounted tissue sections were equilibrated to room temperature, hydrated in PBS for 2 × 5 minutes, permeabilized in 0.1% Triton X-100 in PBS for 20 minutes at room temperature and washed for 2 × 5 minutes in PBS before isolation with a hydrophobic PAP pen (Immedge pen, Vector Laboratories). Nonspecific protein binding sites in sections were blocked by incubation in blocking buffer (75 μl; 0.5% bovine serum albumin (g/ml), 0.3% Tween 20, 15% normal goat/donkey serum (Vector Laboratories) in PBS) in a humidified chamber for 30 minutes at room temperature and then sections were drained and incubated with primary antibody (Supporting Information Table 1) diluted in ADB (15% normal goat serum in place of bovine serum albumin) overnight at 4°C. The following day, slides were washed for 3 × 5 minutes in PBS. Tissue sections were then incubated with secondary antibody diluted in ADB for 1 hour in a hydrated incubation chamber at room temperature. After 1 hour, slides were washed for 3 × 5 minutes in PBS, mounted in Vectorshield mounting medium containing DAPI (Vector Laboratories) and stored at 4°C before microscopic analysis.

Microscopy and Analysis

All fluorescently stained sections were analyzed by an operator blinded to the treatment groups. For immunocytochemistry, all βIII-tubulin$^+$ retinal cells (identified by their staining morphology and referred to from here on as RGC), with or without neurites, were counted in each well, recording the total number of RGC and the number of RGC with neurites. Fluorescently stained cells were analyzed using a Zeiss LSM 700 confocal laser-scanning microscope (Carl Zeiss Inc, Thornwood, NY, https://www.zeiss.com). Neurite outgrowth was measured in images taken at ×20 magnification. Each well was divided into nine equal sectors and the length of the longest neurite of each RGC in each sector was measured using Axiovision software (Carl Zeiss Inc). All experiments were repeated on 3 separate occasions with separate animals. Each of the treatment groups in each of the 3 experimental runs comprised 3 replicate wells containing retinal cells harvested from the same animals.

For immunohistochemistry of retina, RBPMS$^+$ and Brn3a$^+$ were counted in 20 μm-thick sections along a 250 μm linear region of the ganglion cell layer (GCL) either side of the optic nerve (as previously described [39]), imaged using a Zeiss LSM 700 confocal laser-scanning microscope. Six sections per retina and 6 retinae (from 6 different animals) per treatment group were quantified. For immunohistochemistry of the optic nerve, growth associated protein-43$^+$ (GAP-43) axons were counted in 14 μm thick longitudinal sections, imaged using a Zeiss LSM 700 confocal laser-scanning microscope and images composites created using Photoshop CS6 (Adobe Systems, Inc., San Jose, CA, http://www.adobe.com). The number of axons were quantified at 100 μm distance intervals extending distal to the laminin$^+$ crush site, up to a

maximum distance of 1.2 mm. Three sections per optic nerve and 6 optic nerves (from 6 different animals) per treatment group were quantified. The diameter of the nerve was measured at each distance to determine the number of axons/mm width. This value was then used to derive $\sum ad$, the total number of axons extending distance d in an optic nerve with radius r using:

$$\sum ad = \pi r^2 \times \frac{Average\ number\ of\ axons/mm\ width}{Section\ thickness\ (0.015\ mm)}.$$

Statistics

Animal numbers were determined beforehand using a power calculation [40] (Gpower). All statistical tests were performed using SPSS 17.0 (IBM SPSS, Inc., Chicago, IL, http://www.ibm.com) and data presented as mean ± SEM with graphs constructed using Graphpad Prism (La Jolla, CA, https://www.graphpad.com). The Shapiro-Wilkes test was used to ensure all data were normally distributed before parametric testing using a one-way analysis of variance (ANOVA) with a Tukey post hoc test. Statistical differences were considered significant at p values $< .05$.

RESULTS

BMSC Secrete Exosomes

Both human fibroblast and human BMSC secreted exosomes, as detected by electron microscopy and quantified by CD63 ExoELISA (Fig. 2A). Exosomes were visualized using electron microscopy and no observable differences were seen between BMSC and fibroblast exosomes but size differences were when comparing exosomes before and after filtration though a 0.22 μm filter to remove microvesicles. As detected by ELISA, secretion rate was not significantly different between BMSC and fibroblasts. Fibroblasts secreted $1.03 \times 10^9 \pm 1.17 \times 10^8$ exosomes whereas BMSC secreted $1.17 \times 10^9 \pm 1.42 \times 10^8$, measured over a 24-hour time point and normalized to 100,000 cells. Using flow cytometry, we analyzed the surface expression of various CD molecules on exosomes from BMSC and fibroblasts (Fig. 2B). We detected 13 different CD molecules variably expressed on BMSC and/or fibroblast exosomes. In particular, more CD11c$^+$ and CD63$^+$ exosomes were detected on the BMSC exosomes (20.3% ± 8.3%, 81.7% ± 12.3%, respectively) compared to fibroblast exosomes (7.7 ± 0.7, 49.6 ± 2.4, respectively) whereas more CD29$^+$ and CD81$^+$ exosomes were detected on fibroblast exosomes (32.4% ± 0.75%, 39% ± 3.3%, respectively) compared to BMSC exosomes (20.5% ± 1.9%, 15.3% ± 10.6%, respectively). CD1c, CD2, CD3, CD4, CD14, CD20, CD25, CD31, CD40, CD42a, CD45, CD49e, CD56, CD69, CD133/1, CD146, and CD326 were undetectable. Due to the differences in the number of exosomes expressing CD63, exosome counts (Fig. 2A) were normalized using this data.

BMSC-Derived Exosomes Promote Neuroprotection and Neuritogenesis of Cultured Primary RGC

Treatment of RGC cultures with 3×10^9 BMSC EV (exosomes + microvesicles) elicited optimum significant survival (Fig. 3A) of RGC (321 ± 22.3 RGC per well) compared to untreated RGC (121.3 ± 6.2)/3×10^9 fibroblast EV treated RGC (72.3 ± 6.4) and was similar to treatment with 50,000 BMSC (328 ± 24 RGC per well). At higher doses of BMSC EV (1.5×10^{10}, 7.5×10^{10}), RGC
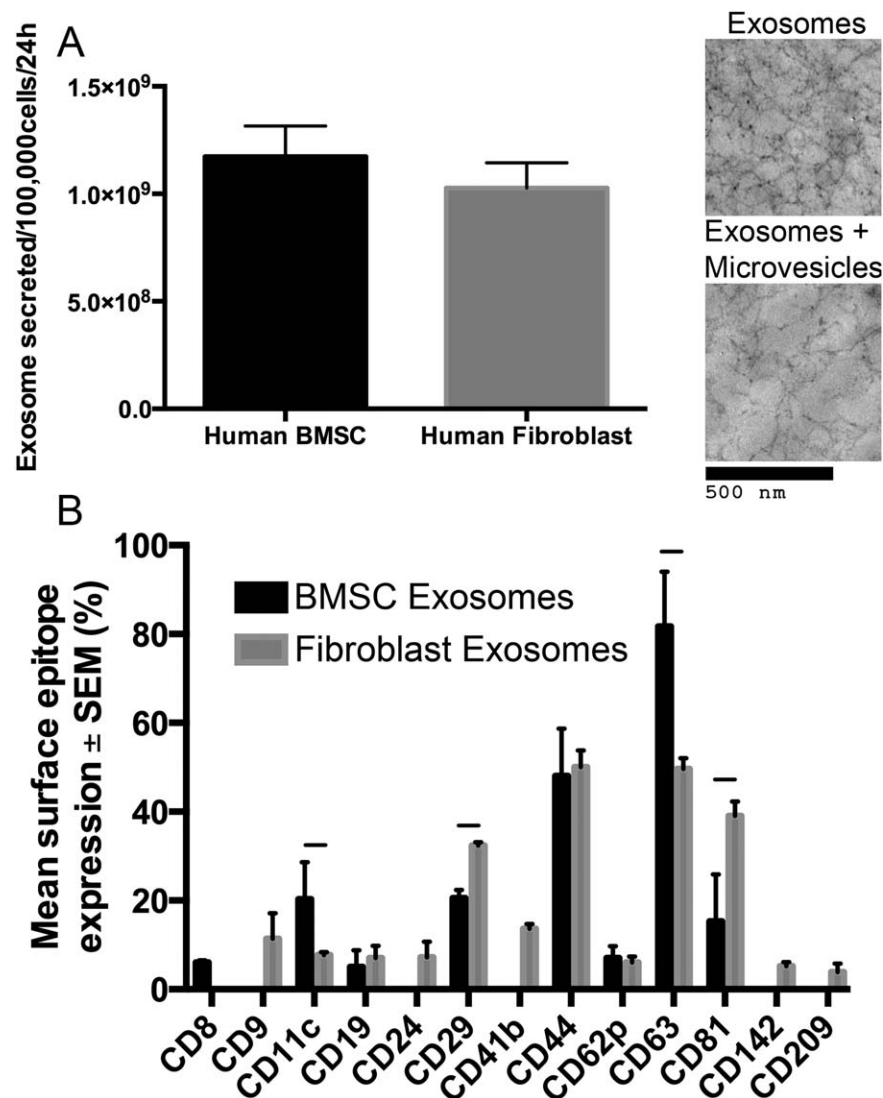
Figure 2. Exosome secretion from fibroblasts and BMSC. **(A)**: The number of exosomes, assayed and quantified by CD63 ExoELISA, secreted by human fibroblasts and human BMSC, given as exosomes per 100,000 cells, per 24 hours. Numbers were corrected to take into account CD63 expression percentage as determined by flow cytometry. No significant difference was found ($p < .05$). **(B)**: The percentage of exosomes that express various CD surface expression markers assayed and quantified using a MACSPlex Exosome Kit (human) in conjunction with flow cytometry. The surface markers CD2, CD3, CD4, CD14, CD25, CD31, CD40, CD42a, CD45, CD49e, CD56, CD69, CD133/1, CD146, and CD326 were not detected in either sample. *Black lines* indicate significant difference ($p < .05$). Abbreviation: BMSC, bone marrow-derived mesenchymal stem cell.

neuroprotection was significantly reduced (202.7 ± 10.7, 58 ± 14.4 RGC per well, respectively) unless microvesicles were first removed from the sample (leaving exosomes), in which case higher doses were still equally neuroprotective (299 ± 24.1, 270.3 ± 47.3 RGC per well, respectively).

Neuritogenesis was measured both as the number of neurite-bearing RGC (Fig. 3B) and the average length of the longest neurites (Fig. 3C). Treatment of RGC cultures with 3×10^9 BMSC EV elicited optimum neuritogenesis of RGC (154 ± 4 RGC with neurites; 114.2 ± 5 μm) compared to untreated RGC (32.3 ± 3.5 RGC with neurites; 43.7 ± 6.9 μm)/3×10^9 fibroblast EV treated RGC (25.7 ± 3.3 RGC with neurites; 45.2 ± 4.1 μm) and was similar to treatment with 50,000 BMSC (166.7 ± 11.3 RGC with neurites; 186.3 ± 21.8 μm). At higher doses of BMSC EV (1.5×10^{10}, 7.5×10^{10}), RGC neuritogenesis was significantly reduced (27.3 ± 4.4, 11.7 ± 3.5 RGC with neurites; 54.8 ± 2.4, 42.7 ± 2 μm,

respectively), unless microvesicles were first removed from the sample (leaving exosomes), in which case higher doses were still equally neuritogenic (128.7 ± 16.0, 109.3 ± 18.8 RGC with neurites; 127.9 ± 5.2, 140.1 ± 15.5 μm, respectively). Increasing or decreasing the number of control fibroblast-derived exosomes/EV did not have any significant effect on neuroprotection and neuritogenesis (data not shown).

BMSC-Derived Exosomes Preserve RNFL THICKNESS following ONC

The thickness of the RNFL is a measure of RGC axonal density and did not change over 21 days in intact animals as well as between groups pre-ONC. In untreated animals, RNFL thickness decreased significantly from 48.2 ± 1.3 μm to 18.0 ± 2.1 μm 21 days after ONC (Fig. 4). In animals receiving BMSC-derived exosomes, RNFL thickness was reduced from 48.4 ± 2.9 μm to 33.8 ± 4.8 μm
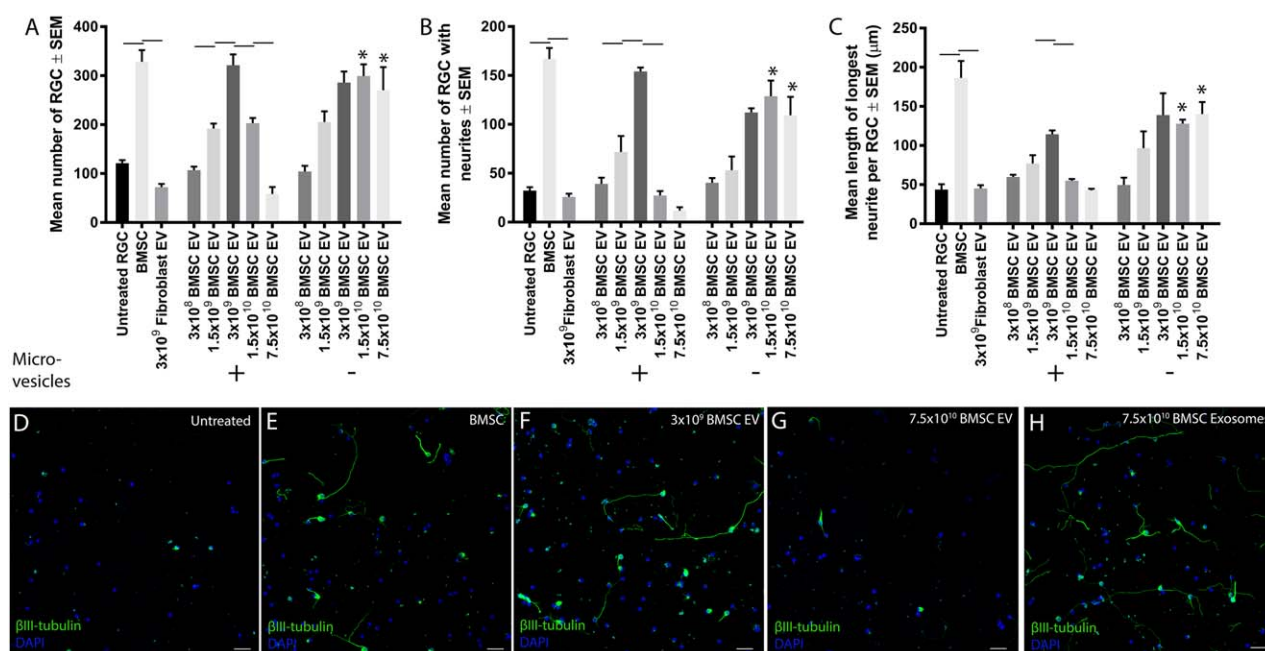
Figure 3. Effects of exosome treatment on RGC neuroprotection and neuritogenesis. The number of RGC **(A)**, number of RGC bearing neurites **(B)** and the length of the longest neurite **(C)** in heterogeneous retinal cultures after treatment with different quantities of EV, before (exosomes + microvesicles) and after (exosomes) filtration. *Black lines* indicate significant difference between groups whereas *asterisks* indicate significant difference between filtered and unfiltered exosomes ($p < .05$). Representative images of heterogeneous retinal cultures either untreated **(D)** or treated with BMSC **(E)**, 3×10^9 BMSC exosomes with microvesicles **(F)**, 7.5×10^{10} BMSC exosomes with microvesicles **(G)** or 7.5×10^{10} BMSC exosomes **(H)**. All images are representative of the entire culture, nine separate culture wells/treatment, with every 3 wells using a different animal (scale bars: 50 μm). Sections were stained for βIII-tubulin (*green*) and DAPI (*blue*). Abbreviations: BMSC EV, bone marrow-derived mesenchymal stem cells extracellular vesicles; RGC, retinal ganglion cells.

21 days after ONC, which was a significantly smaller reduction in comparison to both untreated animals and animals receiving fibroblast-derived exosomes (21.6 ± 1.5 μm). In animals receiving exosomes derived from SiAgo2 transfected BMSC (knockdown confirmed by Western blot; Fig. 4B), RNFL thickness decreased significantly from 46.0 ± 2.2 μm to 22.0 ± 2.2 μm whereas in animals receiving exosomes derived from SiScr transfected BMSC, post-ONC RNFL was, in comparison, significantly higher (32.4 ± 5.3 μm).

BMSC-Derived Exosomes Successfully Integrate and Deliver Cargo to RGC In Vivo

To determine the fate of exosomes after delivery into the vitreous body they were tracked by the internalization of a fluorescent marker (ExoGreen) prior to injection. Fluorescent labeling was seen in the RNFL and GCL in a nonspecific manner. RBPMS$^+$ RGC along with the RNFL and resident cells (morphologically identified as astrocytes) incorporated exosomes and thus were labeled strongly with ExoGreen (Fig. 5B).

BMSC-Derived Exosomes Promote Neuroprotection of RGC Following ONC

ONC induced a significant loss of RBPMS$^+$ and Brn3a$^+$ RGC by day 21 (23.6 ± 7.7 and 29.1 ± 7.8/mm of retina, respectively), compared to intact controls (103.1 ± 6.9 and 75.5 ± 3.9/mm of retina, respectively; Fig. 5). Intravitreal transplantation of 3×10^9 BMSC exosomes provided significant neuroprotection for RBPMS$^+$ and Brn3a$^+$ RGC (73.3 ± 7.8 and 54 ± 8.2/mm of retina, respectively), compared to controls receiving fibroblast exosomes (20 ± 2.2 and 14.3 ± 7.4/mm of retina, respectively). Intravitreal

transplantation of exosomes-derived from SiAgo2 transfected BMSC failed to significantly protect RBPMS$^+$ and Brn3a$^+$ RGC (11.63 ± 1.1 and 4.42 ± 0.4/mm of retina, respectively) whereas exosomes derived from SiScr transfected BMSC were significantly RGC neuroprotective.

BMSC-Derived Exosomes Preserve RGC Function

The amplitude of the pSTR is a measure of RGC function and did not change over 21 days in intact animals as well as between groups pre-ONC (Fig. 6). In untreated animals, pSTR amplitude decreased significantly from 48.7 ± 5.5 μv to 13.7 ± 1.1 μv 21 days after ONC. In animals receiving BMSC-derived exosomes, pSTR amplitude was reduced from 44.3 ± 8.6 μv to 28.6 ± 8.1 μv 21 days after ONC, which was a significantly smaller reduction in comparison to both untreated animals and animals receiving fibroblast-derived exosomes (13.2 ± 3.4 μv). In animals receiving exosomes derived from SiAgo2 transfected BMSC, pSTR amplitude decreased significantly from 45.4 ± 8.7 μv to 20.12 ± 2.9 μv whereas in animals receiving exosomes derived from SiScr BMSC, post-ONC pSTR amplitude was, in comparison, significantly higher (28.7 ± 6.6 μv).

BMSC-Derived Exosomes Promote Regeneration of RGC Axons Following ONC

Intravitreal transplantation of 3×10^9 BMSC exosomes promoted significant regeneration of GAP-43$^+$ axons up to 600 μm from the laminin$^+$ crush site compared to untreated controls/controls receiving fibroblast exosomes (Fig. 7). Intravitreal transplantation of exosomes-derived from SiAgo2 transfected BMSC failed to promote significant regeneration of GAP-43$^+$ axons whereas
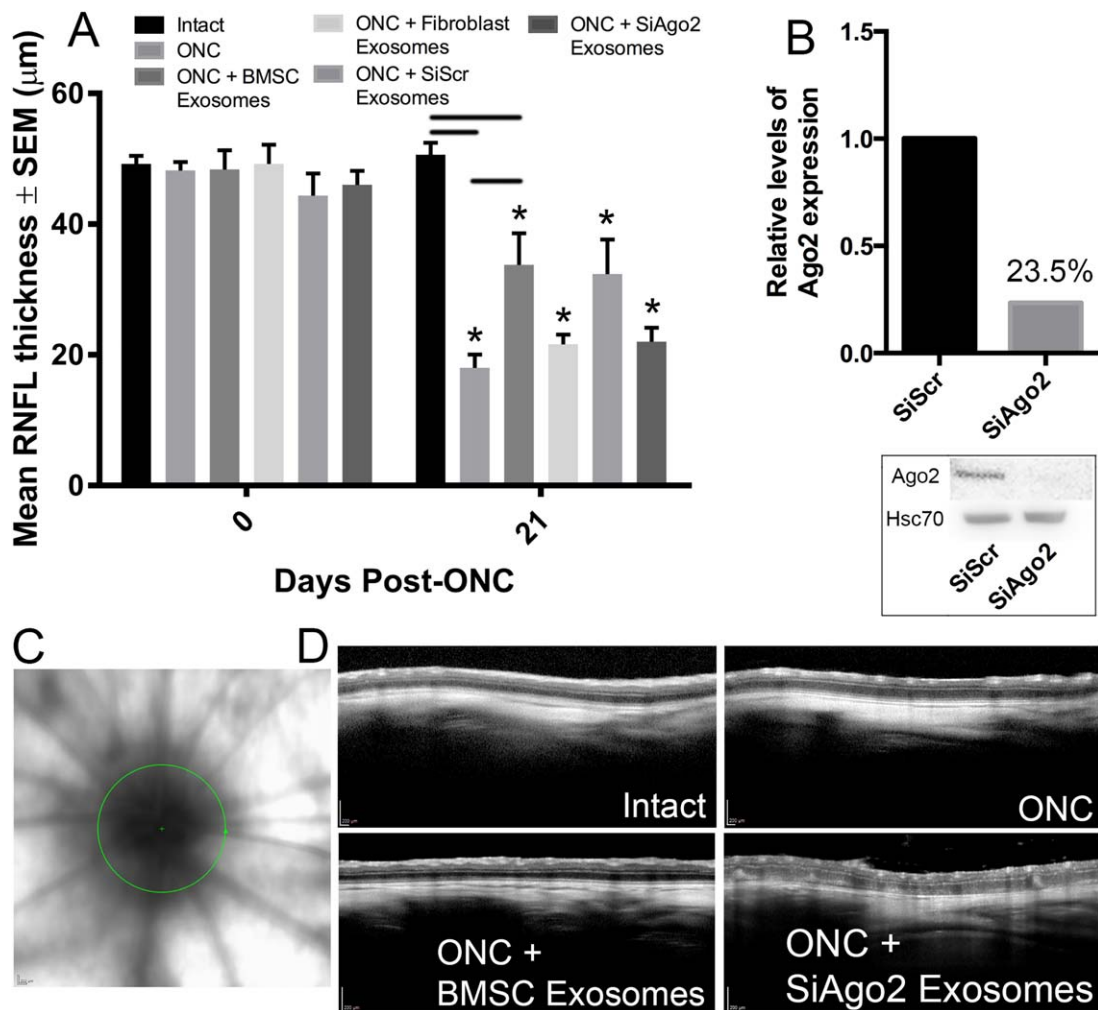
Figure 4. RNFL thickness of rats after ONC and exosome treatment. **(A)**: Graph depicting the mean RNFL thickness (μm) of rats before and 21 days after ONC. *Black lines* indicate significant difference between groups whereas *asterisks* indicate significant difference from the same group pre-ONC ($p < .05$). **(B)**: RNFL measurements were done from a section of retina surrounding the optic nerve head (*green line*). **(C)**: Representative images of retina from Group 1, 2, 3, and 6, as measured by OCT (scale bars: 200 μm). Abbreviations: BMSC, bone marrow-derived mesenchymal stem cells; ONC, optic nerve crush; RNFL, retinal nerve fiber layer.

exosomes derived from SiScr transfected BMSC were significantly RGC axogenic.

DISCUSSION

This study is to our knowledge the first time RGC have been treated with exosomes and the first time BMSC-derived exosomes have been delivered into the eye. Utilizing the ONC model of CNS injury that is characterized by RGC death and a failure of axon regeneration, we demonstrate a significant neuroprotective and axogenic effect afforded by BMSC-derived exosomes as well as the capacity to preserve retinal function. Exosomes successfully deliver their cargo to the inner retina, including the RGC and elicit therapeutic effects through miRNA dependent mechanisms.

RGC are CNS neurons and thus are neither replaceable nor capable of axon regeneration. While BMSC have proven effective as neuroprotective and axogenic agents, it is more clinically translational to purify and use their cell-free active compounds. As exosomes contain proteins, mRNA and miRNA, they possess the potential to not only deliver proteins and translatable mRNA but

also the silencing of genes through RNA interference [41]. They can be isolated relatively easily through simple centrifugation techniques [21] enabling the generation of a cell-free therapy, combining the benefits of BMSC-mediated paracrine repair without the risks [42]. They can also be easily stored and do not proliferate, making the application of specific doses easier. Due to their smaller size, they are also capable of migrating into the GCL from the vitreous (unlike transplanted cells) and delivering their content to the RGC. The surrounding phospholipid bilayer of exosomes protects the contents against degradation and makes them immunologically inert, qualities important for a therapeutic delivery system [43].

Here we show that BMSC secrete exosomes and to similar quantities of that of fibroblast controls. While few studies have monitored exosome secretion rate, our control numbers corroborate those seen in cell lines [44]. For example, a recent study reported secretion rate of 4×10^8 exosomes per 100,000 cells per 24 hours in MCF10A cell lines [45]. Flow cytometry of exosomes revealed two important conclusions. First, there are distinct differences between exosomes from BMSC and fibroblasts and this is reflected in their surface epitope expression. This is
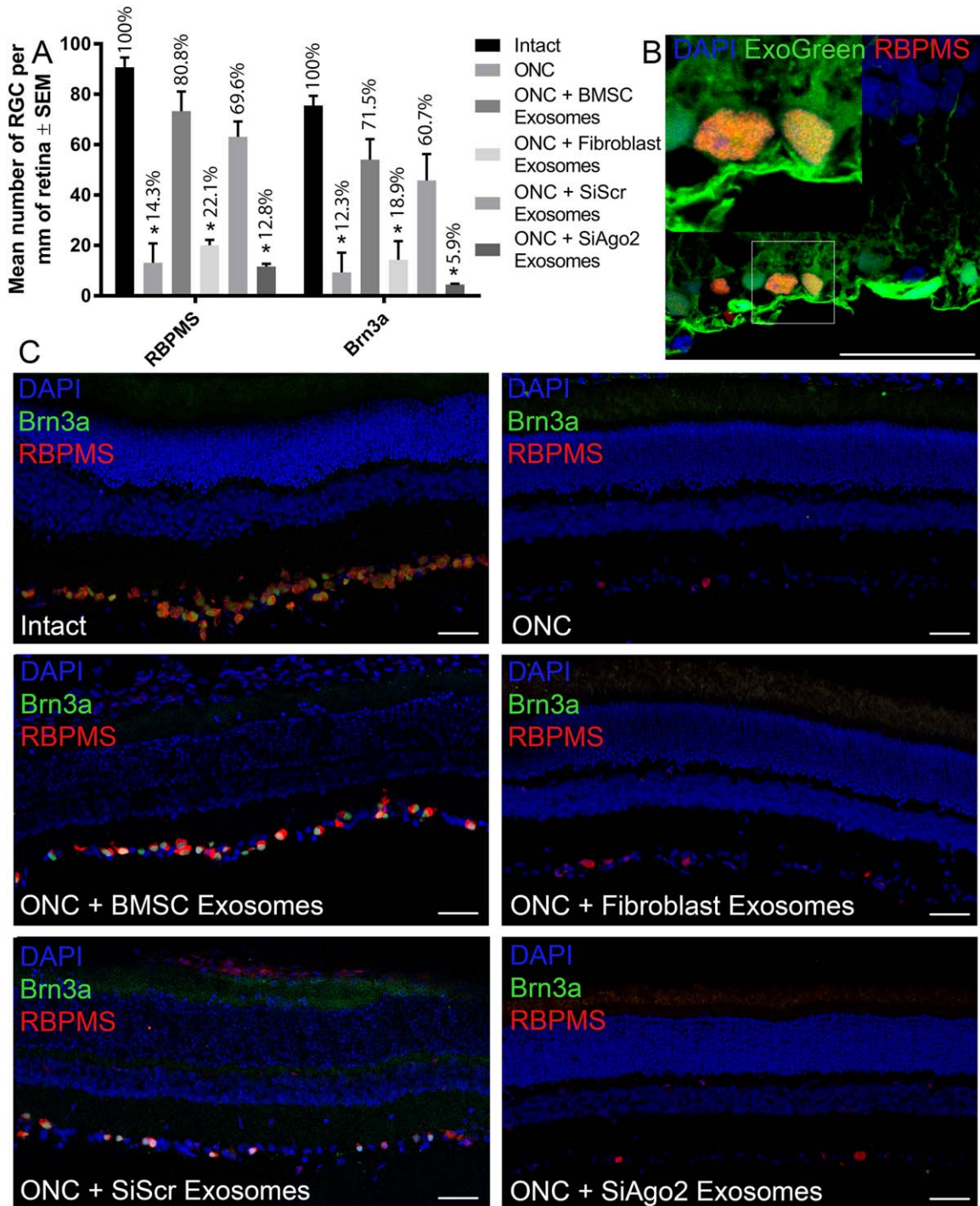
Figure 5. Brn3a^{+} and RBPMS[+] RGC counts in exosome treated retina after ONC. **(A)**: Graph depicting the mean number of Brn3a^{+} and RBPMS[+] RGC in a 1-mm region of retina either side of the optic nerve head. Percentage of surviving RGC in comparison to intact controls is given above each group. *Asterisks* indicate a significant difference from intact, ONC + BMSC Exosomes and ONC + SiScr Exosomes groups ($p < .05$). **(B)**: Image of retina immunohistochemically stained for RBPMS (*red*) from animals injected with ExoGreen labeled exosomes (*green*). **(C)**: Representative images of retina from Group 1 to 6, immunohistochemically stained for Brn3a (green) and RBPMS (*red*). All images show tissue counterstained with the nuclear marker DAPI (*blue;* scale bars: 50 μm*)*. Abbreviations: BMSC, bone marrow-derived mesenchymal stem cells; ONC, optic nerve crush; RGC, retinal ganglion cells.

important to consider when using surface epitopes to quantify exosomes from different cell types Second, exosomes from the same cells express different epitopes, suggesting there may be distinct subtypes of exosomes.

Culture of injured RGC is an effective in vitro model of RGC death and abortive axonal regeneration, and has been used extensively [46, 47] such as demonstrating the neuroprotective and neuritogenic properties of BMSC [7]. Here we have shown that
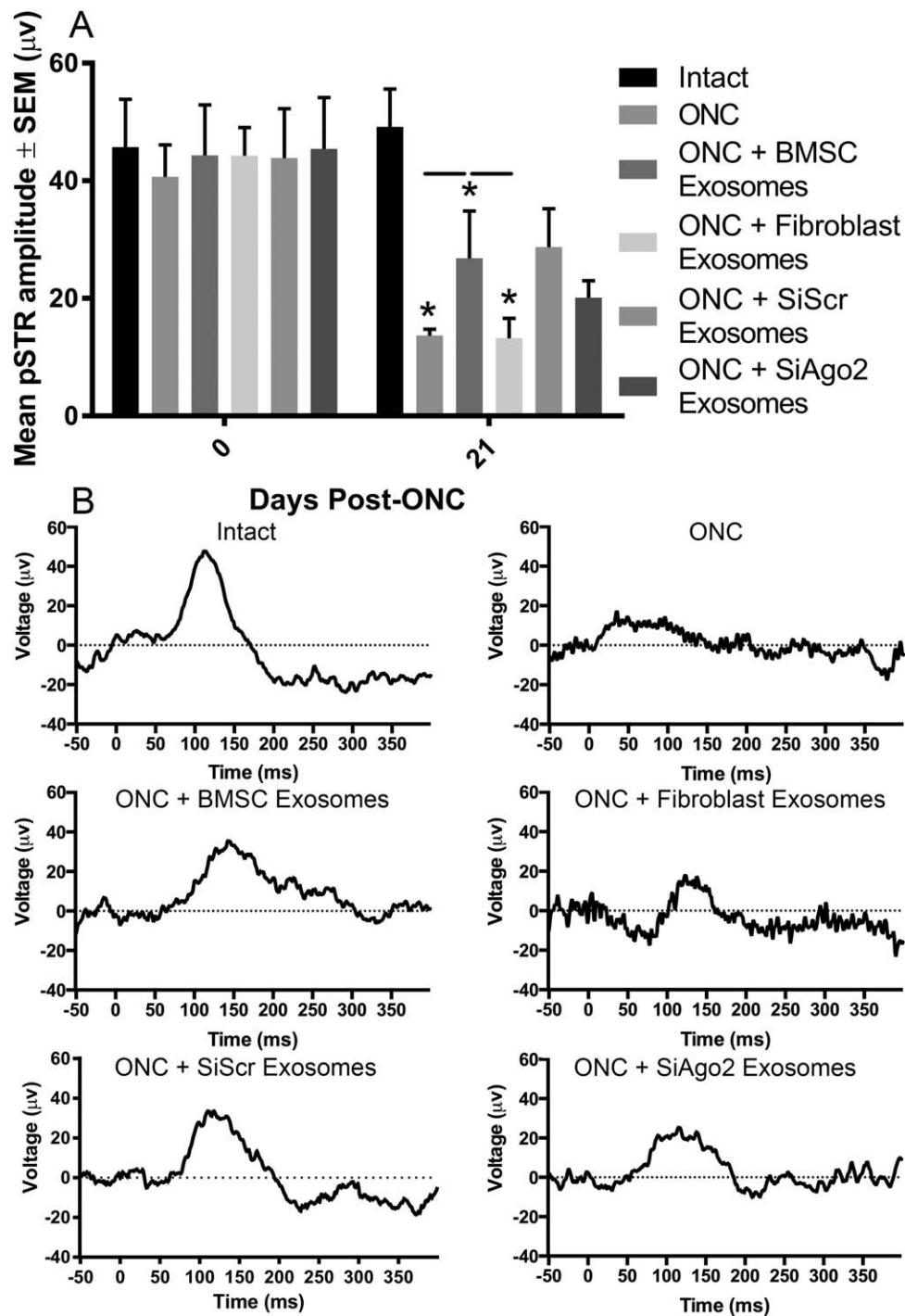
Figure 6. Figure 6: pSTR responses after ONC and exosome treatment. **(A)**: Mean amplitude of pSTR from intact or ONC animals receiving intravitreal exosome treatments after receiving flash intensity of 1×10^{-5} mcd/s. *Black lines* indicate significant difference between groups whereas *asterisks* indicate significant difference from the same group pre-ONC ($p < .05$). **(B)**: Representative traces of observable pSTR from groups 1-6. Abbreviations: ONC, optic nerve crush; pSTR, positive scotopic threshold response.

BMSC can be substituted with BMSC-derived exosomes without a loss in efficacy. Two previous studies have similarly demonstrated a neuritogenic effect of BMSC exosomes on cortical neurons, although survival was not assessed [32, 48]. Interestingly, we found that a negative effect was present at increasing doses of EV and attributed this to microvesicles. Filtration and removal of microvesicles from the samples negated the dose-dependent

negative effect and thus exosomes purified from EV were used for the in vivo experiments. A previous study treating cortical neurons with EV reported similar findings. The study found microvesicles inhibited neuritogenesis whereas exosomes augmented it [48]. In contrast to our study however, authors found that exosome treatment completely overcame the inhibitory properties of microvesicles and were thus still effective in combination. It is possible
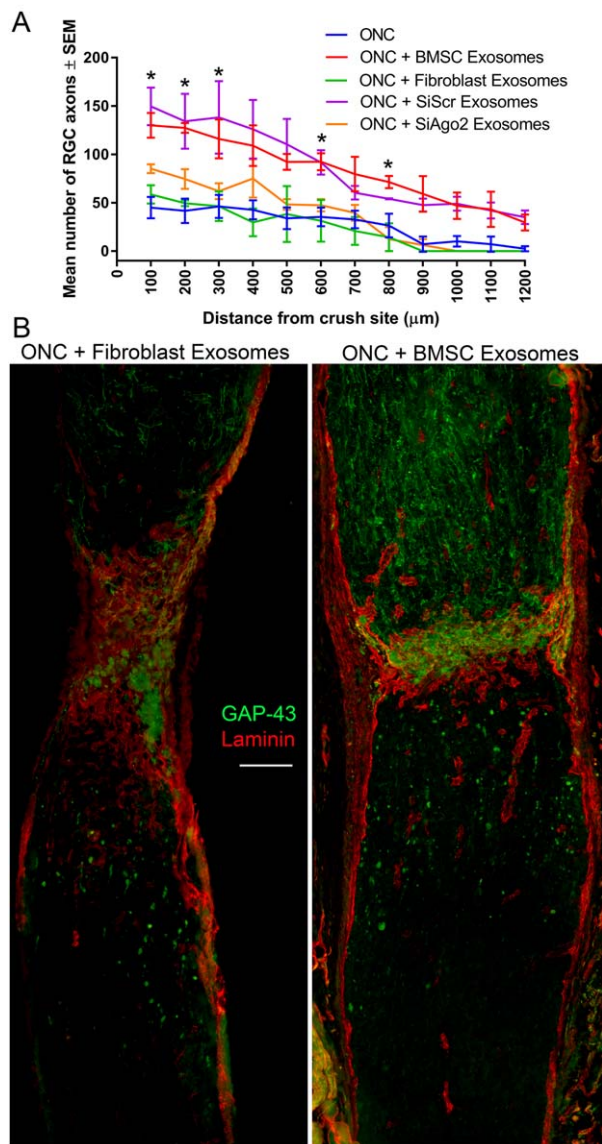
Figure 7. GAP-43+ RGC axon counts in the optic nerve after ONC. **(A):** Graph depicting the mean number of GAP-43+ RGC axons in the optic nerve at 100–1200 μm from the laminin+ crush site. *Asterisks* indicate significant difference between ONC/ONC + fibroblast exosomes and ONC + BMSC exosomes/SiScr exosomes ($p < .05$). **(B):** Representative images of optic nerves immunohistochemically stained for GAP-43 (*green*) and laminin (*red*) from groups 3 and 4 (scale bars: 100 μm). Abbreviations: BMSC, bone marrow-derived mesenchymal stem cells; ONC, optic nerve crush; RGC, retinal ganglion cells.

presence of Brn3a- RGC subtypes [51]), the relative differences between groups remained the similar. Many BMSC do not survive the vitreal transplantation, particular as they lack the capacity to integrate into the retina and thus remain in the vitreous. Therefore, despite actively secreting NTF [7] as well as exosomes, the titres are likely low and diminish with time. In contrast, exosomes were easily isolated, purified and delivered at high doses, potentially explaining why they were significantly more effective at preventing RGC death. It is equally important to recognize that exosomes were delivered 0, 7, and 14 days post-ONC as opposed to previous studies that transplanted BMSC only once on the day of surgery. We chose this treatment regime to partially emulate the continuous secretion of BMSC-derived exosomes.

By labeling the protein cargo of exosomes before intravitreal injection, we were able to track the exosomes and identify which retinal cells they fused with. We found a strong staining consistently through the RNFL and GCL of the retina. Exogreen labeling co-localized with the RNFL, RBPMS+ RGC, and RBPMS− cells morphologically resembling astrocytes. In cortical neuronal cultures, it has been demonstrated that BMSC exosomes integrate into neuronal cell bodies and axons [32]. In an in vivo model of cognitive impairment, intravenous administration of BMSC-derived exosomes led to their integration into both neurons and astrocytes. Since in the present study RGC were not the only target of BMSC exosomes, it is not clear if the therapeutic effect we observed was via a direct effect on the RGC or through astrocyte/müller glia intermediaries.

The significant neuroprotection afforded by BMSC exosomes is corroborated by our OCT and ERG data, demonstrating a significant protection of RGC axons (measured as RNFL thickness) and preservation of RGC function (measured as pSTR amplitude). A residual function was seen in untreated and fibroblast exosome treated control retina after ONC, likely explained by the presence of select subtypes of RGC that are resistant to ONC [52]. However, in BMSC exosome treated retina, over 50% of RGC function was maintained, suggesting a strong effect not only to protect RGC from death but also to retain their function.

We [10] and others [11, 50] have previously demonstrated that intravitreal BMSC treatment promotes moderate regeneration of RGC axons after ONC. The promising neurite outgrowth seen in the present study when retinal cultures were treated with BMSC-derived exosomes was corroborated by their efficacy to promote regeneration of GAP-43+ axons after ONC. The regeneration however was only significant at short distances from the lesion site (<1 mm) limiting its potential at promoting functional reconnection of the visual pathway. The use of BMSC exosomes to promote in vivo axon regeneration is currently untested outside of this study however, previous in vitro studies have demonstrated a neuritogenic property on CNS neurons [32, 48]

As exosomes contain both proteins and miRNA, and studies have reported that both can mediate the therapeutic effect [31], we determined which was the active compound by using SiAgo2. Ago2 regulates the biological function of miRNA [53], is bound to miRNA [54] and its knockdown reduces miRNA quantity within exosomes. [32, 54]. We were able to successfully knockdown Ago2 and demonstrated that BMSC exosomes had a significantly muted effect in promoting RGC neuroprotection, axon regeneration/survival and RGC functional preservation. These data strongly suggest that treating RGC with exosomes is more dependent on miRNA rather than protein. This is corroborated by protein analysis of BMSC exosomes that did not detect any candidate NTF

that with higher doses however, the inhibitory effects of microvesicles may become more pronounced. Equally, it is possible that adult RGC are more resistant to neuritogenesis than cortical neurons and thus more susceptible to the inhibitory properties of microvesicles.

ONC is a reliable model characterized by substantial RGC death and axonal degeneration. We observed the typical 80%–90% RGC loss 21 days after ONC [39, 49] in untreated retina whereas treatment with BMSC-derived exosomes reduced RGC loss to 30%. This is significantly higher neuroprotection than we and others previously observed with BMSC transplants [10, 50]. Although RBPMS stained more RGC than Brn3a (owing to the

among their cargo [22]. In contrast BMSC exosomes contain a variety of miRNA [55–57], many of which their function is currently unknown. One candidate is miR-17-92 which is located within BMSC-derived exosomes [32] and has been found to target and downregulate phosphatase and tensin homolog (PTEN) expression [32], an important suppressor of RGC axonal growth and survival [58, 59]. Similarly, miR-21, which is expressed in umbilical cord MSC-derived exosomes [56] has been shown to regulate PTEN expression [60]. Another candidate miRNA is miR-146a which is expressed in BMSC exosomes [55] and targets the epidermal growth factor receptor (EGFR) mRNA [61]. Activation of EGFR inhibits axon regeneration whereas receptor blockade promotes RGC axon regeneration [47, 62]. Activation of the Akt pathway has also been reported by BMSC-derived exosomes [63], which is a pathway integral to the survival and regeneration of injured RGC [5].

CONCLUSION

We demonstrate for the first time that BMSC-derived exosome offer significant therapeutic benefit to the protection of RGC, an effect mediated by their miRNA rather than protein content. Exosomes offer a cell-free alternative to BMSC therapy, which can be easily isolated, purified and stored. They lack the risk of complications associated with transplanting live cells into the vitreous (immune rejection, unwanted proliferation/differentiation). It is however currently unknown what the ideal timeframe for treatment is, whether a single injection of exosomes is sufficient or weekly/bi-weekly/monthly injections are required. Future work should concentrate on determining the above, as well characterizing the miRNA content of BMSC-derived exosomes and their targets within the known neuroprotective/axogenic pathways to identify candidate miRNA.

AUTHOR CONTRIBUTIONS

B.M.: conception and design, collection and/or assembly of data, data analysis and interpretation, manuscript writing; S.T.: conception and design, data analysis and interpretation, manuscript writing.

DISCLOSURE OF POTENTIAL CONFLICTS OF INTEREST

The authors indicate no potential conflicts of interest.

REFERENCES

1 Friedenstein AJ, Chailakhjan RK, Lalykina KS. The development of fibroblast colonies in monolayer cultures of guinea-pig bone marrow and spleen cells. Cell Tissue Kinet 1970;3: 393–403.

2 Zuk PA, Zhu M, Mizuno H et al. Multilineage cells from human adipose tissue: Implications for cell-based therapies. Tissue Eng 2001;7:211–228.

3 Gronthos S, Mankani M, Brahim J et al. Postnatal human dental pulp stem cells (DPSCs) in vitro and in vivo. Proc Natl Acad Sci USA 2000;97:13625–13630.

4 Kogler G, Sensken S, Airey JA et al. A new human somatic stem cell from placental cord blood with intrinsic pluripotent differentiation potential. J Exp Med 2004;200:123–135.

5 Berry M, Ahmed Z, Lorber B et al. Regeneration of axons in the visual system. Restor Neurol Neurosci 2008;26:147–174.

6 Mead B, Berry M, Logan A et al. Stem cell treatment of degenerative eye disease. Stem Cell Res 2015;14:243–257.

7 Mead B, Logan A, Berry M et al. Paracrine-mediated neuroprotection and neuritogenesis of axotomised retinal ganglion cells by human dental pulp stem cells: comparison with human bone marrow and adipose-derived mesenchymal stem cells. PLoS One 2014;9:e109305.

8 Mead B, Logan A, Berry M et al. Dental pulp stem cells, a paracrine-mediated therapy for the retina. Neural Regen Res 2014;9:577–578.

9 Levkovitch-Verbin H, Sadan O, Vander S et al. Intravitreal injections of neurotrophic factors secreting mesenchymal stem cells are neuroprotective in rat eyes following optic nerve transection. Invest Ophthalmol Vis Sci 2010;51:6394–6400.

10 Mead B, Logan A, Berry M et al. Intravitreally transplanted dental pulp stem cells promote neuroprotection and axon regeneration of retinal ganglion cells after optic nerve injury. Invest Ophthalmol Vis Sci 2013;54: 7544–7556.

11 Tan HB, Kang X, Lu SH et al. The therapeutic effects of bone marrow mesenchymal stem cells after optic nerve damage in the adult rat. Clin Interv Aging 2015;10:487–490.

12 Zwart I, Hill AJ, Al-Allaf F et al. Umbilical cord blood mesenchymal stromal cells are neuroprotective and promote regeneration in a rat optic tract model. Exp Neurol 2009;216: 439–448.

13 Mead B, Hill LJ, Blanch RJ et al. Mesenchymal stromal cell-mediated neuroprotection and functional preservation of retinal ganglion cells in a rodent model of glaucoma. Cytotherapy 2016; 18:487–496.

14 Emre E, Yuksel N, Duruksu G et al. Neuroprotective effects of intravitreally transplanted adipose tissue and bone marrow-derived mesenchymal stem cells in an experimental ocular hypertension model. Cytotherapy 2015;17:543–559.

15 Johnson TV, Bull ND, Hunt DP et al. Neuroprotective effects of intravitreal mesenchymal stem cell transplantation in experimental glaucoma. Invest Ophthalmol Vis Sci 2010;51:2051–2059.

16 Yu S, Tanabe T, Dezawa M et al. Effects of bone marrow stromal cell injection in an experimental glaucoma model. Biochem Biophys Res Commun 2006;344:1071–1079.

17 Johnson TV, Dekorver NW, Levasseur VA et al. Identification of retinal ganglion cell neuroprotection conferred by platelet-derived growth factor through analysis of the mesenchymal stem cell secretome. Brain 2014137: 503–519.

18 Zhao Y, Gibb SL, Zhao J et al. Wnt3a, a Protein secreted by mesenchymal stem cells is neuroprotective and promotes neurocognitive recovery following traumatic brain injury. STEM CELLS 2016;34:1263–1272.

19 Johnson TV, Bull ND, Martin KR. Identification of barriers to retinal engraftment of transplanted stem cells. Invest Ophthalmol Vis Sci 2010; 51(: 960–970.

20 Pan BT, Johnstone RM. Fate of the transferrin receptor during maturation of sheep reticulocytes in vitro: Selective externalization of the receptor. Cell 1983;33: 967–978.

21 Thery C, Amigorena S, Raposo G et al. Isolation and characterization of exosomes from cell culture supernatants and biological fluids. Curr Protoc Cell Biol 2006;3:22.

22 Kim HS, Choi DY, Yun SJ et al. Proteomic analysis of microvesicles derived from human mesenchymal stem cells. J Proteome Res 2012;11: 839–849.

23 Valadi H, Ekstrom K, Bossios A et al. Exosome-mediated transfer of mRNAs and microRNAs is a novel mechanism of genetic exchange between cells. Nat Cell Biol 2007;9: 654–U72.

24 Kosaka N, Yoshioka Y, Fujita Y et al. Versatile roles of extracellular vesicles in cancer. J Clin Invest 2016;126:1163–1172.

25 Heusermann W, Hean J, Trojer D et al. Exosomes surf on filopodia to enter cells at endocytic hot spots, traffic within endosomes, and are targeted to the ER. J Cell Biol 2016;213:173–184.

26 Lai RC, Arslan F, Tan SS et al. Derivation and characterization of human fetal MSCs: An alternative cell source for large-scale production

of cardioprotective microparticles. J Mol Cell Cardiol 2010;48:1215–1224.

27 Chen TS, Lai RC, Lee MM et al. Mesenchymal stem cell secretes microparticles enriched in pre-microRNAs. Nucleic Acids Res 2010; 38:215–224.

28 Timmers L, Lim SK, Arslan F et al. Reduction of myocardial infarct size by human mesenchymal stem cell conditioned medium. Stem Cell Res 2007;1:129–137.

29 Lai RC, Arslan F, Lee MM et al. Exosome secreted by MSC reduces myocardial ischemia/reperfusion injury. Stem Cell Res 2010;4: 214–222.

30 Arslan F, Lai RC, Smeets MB et al. Mesenchymal stem cell-derived exosomes increase ATP levels, decrease oxidative stress and activate PI3K/Akt pathway to enhance myocardial viability and prevent adverse remodeling after myocardial ischemia/reperfusion injury. Stem Cell Res 2013;10:301–312.

31 Katsuda T, Ochiya T. Molecular signatures of mesenchymal stem cell-derived extracellular vesicle-mediated tissue repair. Stem Cell Res Ther 2015;6:212.

32 Zhang Y, Chopp M, Liu XS et al. Exosomes derived from mesenchymal stromal cells promote axonal growth of cortical neurons. Mol Neurobiol 2016. [Epub ahead of print]. doi:10.1007/s12035-016-9851-0

33 Xin H, Li Y, Cui Y et al. Systemic administration of exosomes released from mesenchymal stromal cells promote functional recovery and neurovascular plasticity after stroke in rats. J Cereb Blood Flow Metab 2013;33: 1711–1715.

34 Zhang Y, Chopp M, Meng Y et al. Effect of exosomes derived from multipluripotent mesenchymal stromal cells on functional recovery and neurovascular plasticity in rats after traumatic brain injury. J Neurosurg 2015; 122:856–867.

35 Nakano M, Nagaishi K, Konari N et al. Bone marrow-derived mesenchymal stem cells improve diabetes-induced cognitive impairment by exosome transfer into damaged neurons and astrocytes. Sci Rep 2016;6:24805.

36 Sullivan KF. Structure and utilization of tubulin isotypes. Ann Rev of Cell Biolo 1988;4: 687–716.

37 Suggate EL, Ahmed Z, Read ML et al. Optimisation of siRNA-mediated RhoA silencing in neuronal cultures. Mol Cell Neurosci 2009;40:451–462.

38 Berry M, Carlile J, Hunter A. Peripheral nerve explants grafted into the vitreous body

of the eye promote the regeneration of retinal ganglion cell axons severed in the optic nerve. J Neurocytol 1996;25:147–170.

39 Mead B, Thompson A, Scheven BA et al. Comparative evaluation of methods for estimating retinal ganglion cell loss in retinal sections and wholemounts. PLoS One 2014;9: e110612.

40 Faul F, Erdfelder E, Lang AG et al. G*Power 3: A flexible statistical power analysis program for the social, behavioral, and biomedical sciences. Behav Res Methods 2007; 39:175–191.

41 Ching RC, Kingham PJ. The role of exosomes in peripheral nerve regeneration. Neural Regen Res 2015;10:743–747.

42 Sun L, Xu R, Sun X et al. Safety evaluation of exosomes derived from human umbilical cord mesenchymal stromal cell. Cytotherapy 2016;18:413–422.

43 Sun DM, Zhuang XY, Zhang SQ et al. Exosomes are endogenous nanoparticles that can deliver biological information between cells. Adv Drug Deliv Rev 2013;65:342–347.

44 Sinha S, Hoshino D, Hong NH et al. Cortactin promotes exosome secretion by controlling branched actin dynamics. J Cell Biol 2016; 214:197–213.

45 Chiu YJ, Cai W, Shih YR et al. A single-cell assay for time lapse studies of exosome secretion and cell behaviors. Small 2016;12: 3658–3666.

46 Lorber B, Berry M, Logan A. Different factors promote axonal regeneration of adult rat retinal ganglion cells after lens injury and intravitreal peripheral nerve grafting. J Neurosci Res 2008;86:894–903.

47 Douglas MR, Morrison KC, Jacques SJ et al. Off-target effects of epidermal growth factor receptor antagonists mediate retinal ganglion cell disinhibited axon growth. Brain 2009;132:3102–3121.

48 Lopez-Verrilli MA, Caviedes A, Cabrera A et al. Mesenchymal stem cell-derived exosomes from different sources selectively promote neuritic outgrowth. Neuroscience 2016; 320:129–139.

49 Berkelaar M, Clarke DB, Wang YC et al. Axotomy results in delayed death and apoptosis of retinal ganglion cells in adult rats. J Neurosci 1994;14:4368–4374.

50 Mesentier-Louro LA, Zaverucha-do-Valle C, da Silva-Junior AJ et al. Distribution of mesenchymal stem cells and effects on neuronal survival and axon regeneration after optic

nerve crush and cell therapy. PLoS One 2014; 9: e110722.

51 Mead B, Tomarev S. Evaluating retinal ganglion cell loss and dysfunction. Exp Eye Res 2016;151: 96–106.

52 Duan X, Qiao M, Bei F et al. Subtype-specific regeneration of retinal ganglion cells following axotomy: Effects of osteopontin and mTOR signaling. Neuron 2015;85:1244–1256.

53 Ha M, Kim VN. Regulation of microRNA biogenesis. Nat Rev Mol Cell Biol 2014;15: 509–524.

54 Guduric-Fuchs J, O'Conner A, Camp B et al. Selective extracellular vesicle-mediated export of an overlapping set of microRNAs from multiple cell types. BMC Genomics 2012; 13: 357.

55 Baglio SR, Rooijers K, Koppers-Lalic D et al. Human bone marrow- and adipose-mesenchymal stem cells secrete exosomes enriched in distinctive miRNA and tRNA species. Stem Cell Res Ther 2015;6:127.

56 Qian X, Xu C, Fang S et al. Exosomal microRNAs derived from umbilical mesenchymal stem cells inhibit Hepatitis C virus infection. Stem Cells Transl Med 2016;5:1190–203.

57 Eirin A, Riester SM, Zhu XY et al. MicroRNA and mRNA cargo of extracellular vesicles from porcine adipose tissue-derived mesenchymal stem cells. Gene 2014;551: 55–64.

58 Park KK, Liu K, Hu Y et al. Promoting axon regeneration in the adult CNS by modulation of the PTEN/mTOR pathway. Science 2008;322: 963–966.

59 Berry M, Ahmed Z, Morgan-Warren P et al. Prospects for mTOR-mediated functional repair after central nervous system trauma. Neurobiol Dis 2016; 85:99–110.

60 Meng F, Henson R, Wehbe-Janek H et al. MicroRNA-21 regulates expression of the PTEN tumor suppressor gene in human hepatocellular cancer. Gastroenterology 2007;133: 647–658.

61 Katakowski M, Buller B, Zheng X et al. Exosomes from marrow stromal cells expressing miR-146b inhibit glioma growth. Cancer Lett 2013;335: 201–204.

62 Koprivica V, Cho KS, Park JB et al. EGFR activation mediates inhibition of axon regeneration by myelin and chondroitin sulfate proteoglycans. Science 2005;310:106–110.

63 Gu H, Ji R, Zhang X et al. Exosomes derived from human mesenchymal stem cells promote gastric cancer cell growth and migration via the activation of the Akt pathway. Mol Med Rep 2016;14:3452–3458.

See www.StemCellsTM.com for supporting information available online.